



Cite this: DOI: 10.1039/c5cc00476d

Received 17th January 2015,  
Accepted 4th February 2015

DOI: 10.1039/c5cc00476d

www.rsc.org/chemcomm

# Assembly of twisted luminescent architectures based on acenaphtho[1,2-*k*]fluoranthene derivatives†

Liang Han, Yuewei Zhang, Weiping Chen, Xiao Cheng, Kaiqing Ye, Jingying Zhang\* and Yue Wang\*

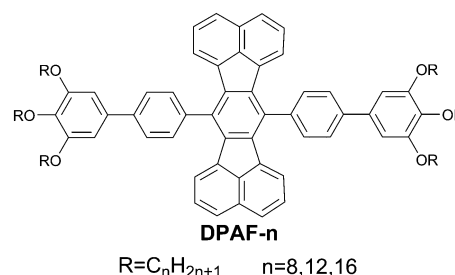
**Acenaphtho[1,2-*k*]fluoranthene derivatives DPAF-*n* as new building blocks for one-dimensional (1D) structure assembly have been developed and employed to fabricate luminescent twisted nano/micro-wires; and the DPAF rigid core attached *via* flexible alkyl chains with suitable lengths is critical for the formation of twisted architectures.**

Among the attractive one-dimensional (1D) architectures, twisted and helical nano/micro-wires and ribbons based on organic functional molecules are the most representative candidates for a better understanding of some life substances and fabrication of optoelectronic devices.<sup>1</sup> Generally, the twisted and helical nano/micro-structures were constructed by assembling the molecules with chiral groups such as peptides,<sup>2</sup> sugar-based derivatives,<sup>3</sup>  $\pi$ -conjugant oligomers<sup>4</sup> and so on.<sup>5</sup> Fabrication based on chiral building blocks is a popular and efficient approach to achieve twisted and helical wires and ribbons. Nevertheless, assembling achiral organic molecules into twisted and helical nano/micro-structures has become a hot topic in the area of supramolecular chemistry recently. Achiral molecules such as phthalocyanines,<sup>6</sup> perylene bisimides,<sup>7</sup> quinacridones<sup>8</sup> and so on<sup>9</sup> have been employed as building blocks to fabricate twisted and helical structures by intermolecular hydrogen bonding and  $\pi$ - $\pi$  stacking interactions. These organic functional molecules with extended  $\pi$ -conjugated aromatic systems endow their assembly systems with unique catalysis,<sup>10</sup> biomaterials<sup>11</sup> and optoelectronic<sup>12</sup> properties. Therefore, it is still an important issue to develop new building blocks for the construction of twisted or helical structures with desired characteristics.

7,14-Diphenylacenaphtho[1,2-*k*]fluoranthene (DPAF) is an extended and fused-ring molecule composed of five- and

six-membered  $\pi$ -conjugation systems. The special structural characteristic suggested that DPAF based molecules have promising luminescence and semiconducting properties.<sup>13</sup> Therefore, DPAF is considered to be a desirable building block to construct functional molecules for supramolecular assembly. In this communication three molecules **DPAF-*n*** (*n* = 8, 12, 16) (Fig. 1) were designed and synthesized by introducing two phenyl groups with alkyl chains to the DPAF skeleton. **DPAF-*n*** molecules possess unique molecular structure and functional characteristics which are as follows: (i) the cross type geometry constructed by a *p*-quinquephenyl and acenaphtho[1,2-*k*]fluoranthene moieties that form the rigid core; (ii) the distinctive and large  $\pi$ -conjugated system suggesting promising emission and semiconducting properties; (iii) the **DPAF-*n*** structure features a rigid central core and flexible side alkyl chains allowing formation by supramolecular assembly. **DPAF-*n*** molecules, which are remarkably different from the reported organic molecules for the assembly of twisted or helical structures,<sup>6–9</sup> represent a new classical building block for the fabrication of functional nano- and micro-materials.

**DPAF-*n*** were synthesized using Suzuki cross-coupling reactions between 7,14-bis[4-bromophenyl]acenaphtho[1,2-*k*]fluoranthene and 3,4,5-trialkylxyphenylboronic acid (Scheme S1, ESI†). To investigate the assembly properties of **DPAF-*n*** molecules, the phase transfer method based on a variety of binary solvents systems was employed. **DPAF-*n*** samples were dissolved in good solvents such as dioxane, chloroform, toluene and tetrahydrofuran. Then the

Fig. 1 Molecular structures of **DPAF-*n***.

State Key Laboratory of Supramolecular Structure and Materials,  
College of Chemistry, Jilin University, Changchun 130012, P. R. China.  
E-mail: zhangjingying@jlu.edu.cn, yuewang@jlu.edu.cn; Fax: +86-431-85193421;  
Tel: +86-431-85168484

† Electronic supplementary information (ESI) available: Synthetic procedures and characterization data; additional emission spectra, XRD patterns, crystal data, fluorescence microscopy, FESEM images. CCDC 1043332. For ESI and crystallographic data in CIF or other electronic format see DOI: 10.1039/c5cc00476d

**DPAF-*n*** solution was added into test tubes, and sequentially a poor solvent such as methanol, ethanol and isopropanol was carefully covered on the top surface of the **DPAF-*n*** solution. Slow diffusion of the poor solvent into the **DPAF-*n*** solution resulted in 1D nano- or micro-materials with the luminescence characteristic in the interlayer between the good and the poor solvent phases.

Well distributed microwires with a twisted morphology based on **DPAF-12** were obtained in the interlayer between dioxane solution of **DPAF-12** (1 mg mL<sup>-1</sup>) and ethanol (Fig. 2a and c). The twisted microwires were as long as several micrometres. Their width and pitch were 2–3 μm and 30–40 μm, respectively, as demonstrated using fluorescence microscopy and FESEM (field emission scanning electron microscopy) images. Both right- and left-handed twisted wires were obtained and twisted samples were racemic mixtures in this study, which was attributed to the absence of a chiral center in the molecules. The morphologies of the twisted wires displayed obviously concentration dependent characteristics. Upon decreasing the concentration of the **DPAF-12** dioxane solution, the width and the pitch of the generated twisted microwires reduced successively (Fig. 2b, d and e). When the concentration reached 0.05 mg mL<sup>-1</sup>, the twisted microwires formed accompanied by a few straight needle-like crystalline wires (Fig. 2f).

Similar **DPAF-12** based twisted microstructures could be also generated from other double layer solvent systems such as chloroform solution–methanol, chloroform solution–ethanol, THF solution–ethanol and chloroform solution–isopropanol with different morphologies, lengths, widths and pitches (Fig. S1, ESI†). On the other hand, by precisely regulating the composition and ratio of the mixture solvent, the twisted architectures could be

achieved through slow evaporation of **DPAF-12** solution (Fig. S2 and S3, ESI†).

The morphologies of the obtained microstructures are sensitive to the polarity of the chosen “poor” solvent for the phase transfer methodology. In dioxane solution of the **DPAF-12**–methanol system, although the twisted wires were prepared, their morphologies were not well-defined (Fig. S4, ESI†). When isopropanol was employed as the “poor” solvent, whose polarity is lower, large numbers of crystalline straight ribbons were generated in the interlayer between dioxane solution and isopropanol solvent (Fig. S5, ESI†). The fluorescence of straight needle-like ribbons showed significant blue-shifts compared with the twisted microwires that formed in dioxane solution–ethanol system. For the same organic compound that may adopt flexible molecular conformation or configuration, the different solvent media may result in various types of molecular packing and crystalline phases (namely polymorphs).<sup>14</sup> The aggregated structures of organic molecules are strongly dependent on the intermolecular interactions.<sup>15</sup> The solubility of **DPAF-12** in various solvents is different, which may induce the generation of aggregated states based on distinct intermolecular interactions. Therefore, the **DPAF-12** molecules with six long alkyl chains should take different configurations and intermolecular interaction in different solvent systems, which can result in the formation of the nano- or micro-structures with different morphologies and luminescence properties. So far, a precise mechanism for the result in this study remains unclear and some detailed investigation should be performed in the future.

To check the assembly properties of DPAF derivatives with different lengths of alkyl chains, **DPAF-16** and **DPAF-8** were used as building blocks to fabricate nano/micro-structures. Indeed, the lengths of the alkyl chains have a dramatic effect on the morphologies of the resulted architectures composed of DPAF derivatives. When compound **DPAF-16** with longer alkyl chains was employed as building blocks for molecular assembly, the individual twisted wires and twisted wire bundles were generated (Fig. 3a) in the interlayer of the chloroform solution (1 mg mL<sup>-1</sup>)–methanol binary solvent system. FESEM microscopy images illustrated the width and pitch of the single twisted wires was about 100 nm and several tens of nanometers, respectively, which were much smaller than those of **DPAF-12** microwires prepared using the same procedure. Under identical conditions except that methanol was replaced by ethanol, most of the resulting 1D ribbons presented wider distribution in dimension and only a small amount of twisted wires were observed (Fig. 3b). Carefully regulating the concentration and solvent media of **DPAF-16** in solution has not led to the formation of well-defined twisted wires (Fig. S6–S9, ESI†).

For compound **DPAF-8** with shorter alkyl chains, non-twisted architectures were dominant in the resulting samples (Fig. 3c and d). The twisted structure was only obtained in the phase transfer system of dioxane solution (0.05 mg mL<sup>-1</sup>)–methanol (Fig. S10, ESI†). It is worth noting that **DPAF-8** molecules easily assembled into flat thin emissive crystals with a smooth surface (Fig. S11, ESI†) by phase transfer (chloroform solution (1 mg mL<sup>-1</sup>)–methanol) or slow evaporation of dioxane solution (1 mg mL<sup>-1</sup>) (Fig. S11, ESI†).

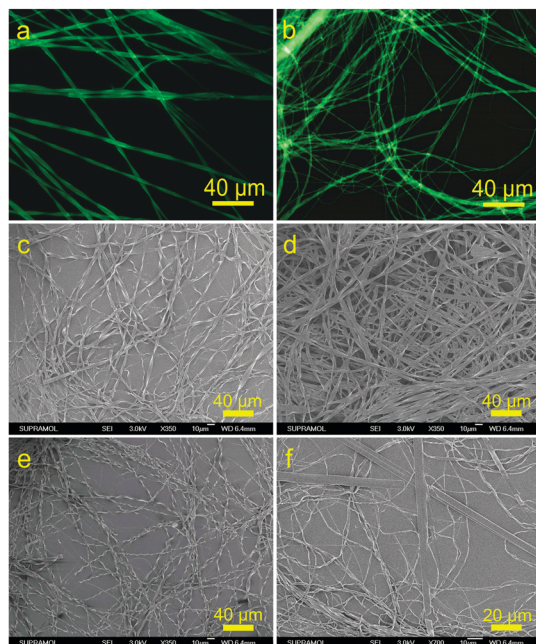


**Fig. 2** Fluorescence microscopy and FESEM images of **DPAF-12** microstructures prepared by phase transfer method from ethanol and dioxane solutions at different concentrations: (a, c) 1 mg mL<sup>-1</sup>; (d) 0.5 mg mL<sup>-1</sup>; (b, e) 0.1 mg mL<sup>-1</sup>; (f) 0.05 mg mL<sup>-1</sup>.

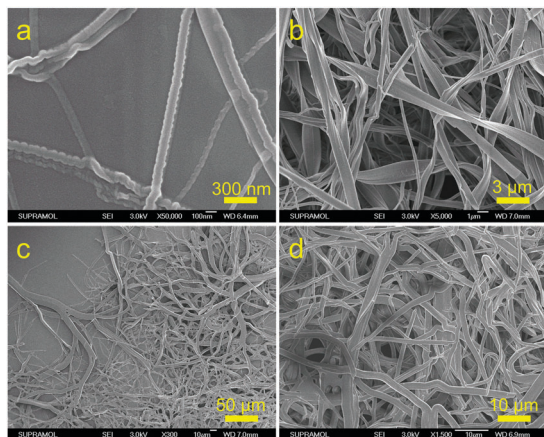


**Fig. 3** FESEM images: (a) **DPAF-16** twisted nanowires prepared from the chloroform solution ( $1 \text{ mg mL}^{-1}$ )–methanol system; (b) **DPAF-16** microribbons prepared from chloroform solution ( $1 \text{ mg mL}^{-1}$ )–ethanol system; (c) **DPAF-8** branched structures prepared from THF solution ( $1 \text{ mg mL}^{-1}$ )–methanol system; (d) **DPAF-8** flat micro-ribbons prepared from dioxane solution ( $1 \text{ mg mL}^{-1}$ )–methanol system using the phase transfer method.

The emission spectra of **DPAF-12** samples in different states are illustrated in Fig. 4. The twisted and flexible wires prepared from dioxane solution of **DPAF-12**–methanol or ethanol systems showed very similar luminescence properties. The emission maxima ( $\lambda_{\text{em}}$ ) at 526 nm and photoluminescence quantum yields ( $\Phi_{\text{F}}$ ) of 0.18 were recorded for the two samples. The crystal powder sample of **DPAF-12** precipitated from chloroform solution displayed very similar emission characteristics ( $\lambda_{\text{em}} = 527 \text{ nm}$ ,  $\Phi_{\text{F}} = 0.19$ ) to twisted wires. The **DPAF-12** straight ribbons generated in the interlayer between dioxane solution and isopropanol demonstrated a much shorter emission maximum (504 nm) and higher photoluminescence quantum yield (0.62) compared with twisted and flexible wires. The emission properties of the straight ribbons were quite similar to those of **DPAF-12**

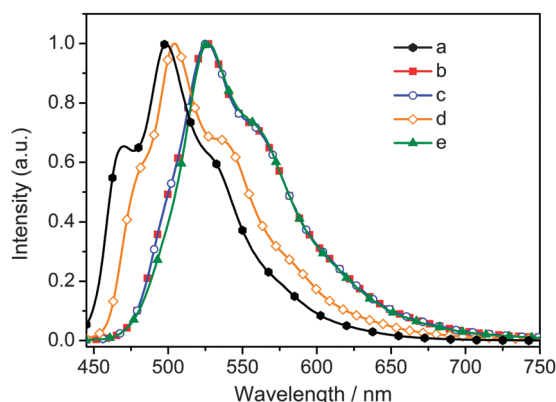


**Fig. 4** Fluorescence spectra of **DPAF-12** based samples: (a) dilute solution in dioxane ( $0.1 \text{ mg mL}^{-1}$ ); (b) microwires prepared from dioxane solution ( $1 \text{ mg mL}^{-1}$ )–methanol system by phase transfer method; (c) twisted microwires prepared from dioxane solution ( $1 \text{ mg mL}^{-1}$ )–ethanol system using the phase transfer method; (d) needle-like crystalline ribbons prepared from dioxane solution ( $1 \text{ mg mL}^{-1}$ )–isopropanol by phase transfer method; (e) solids in the powder state.

dilute solution. To understand the above emission phenomena, powder X-ray diffraction (XRD) measurements were performed (Fig. S12, ESI†). The twisted and flexible wires showed similar XRD patterns to the crystal powder sample, suggesting that these three samples belong to the same crystalline phase. The patterns were indexed (part of indexing peaks are marked in Fig. S12c, ESI†) and the calculated packing period distance is around  $15.2 \text{ \AA}$  reflecting the (100) crystal plane. For straight ribbons, the calculated packing period distance is as large as  $22.213 \text{ \AA}$ . The longer packing period distance means relatively loose molecular packing, which can enhance the emission. In contrast, the dense molecular packing can lead to self-absorption, which induced emission quenching.<sup>15</sup> The XRD analysis results provide rational explanation for the emission behavior of the **DPAF-12** solid samples.

To figure out molecular packing and assembly characteristics of **DPAF-*n*** series building blocks, the single crystal structure of **DPAF-8** was investigated. In **DPAF-8** crystal the molecules adopt two different conformations, namely S and I type conformations (Fig. 5a and Fig. S13a, ESI†). For S type molecules, the side alkyl chains show a sharp bend feature, while for I type molecules, the alkyl chains adopt a relatively slight bend orientation. The S and I type molecules array alternately to form the molecular chains, which pack together to result in the architecture of crystal. Along the  $[10\bar{1}]$  direction, the molecules were linked together by intermolecular  $\text{C-H} \cdots \pi$  interactions between alkyl chains and aromatic cores (Fig. 5b and Fig. S13c, ESI†). Along the  $[101]$  direction, the molecules stack each other based on the intermolecular  $\text{C-H} \cdots \pi$  interactions between adjacent molecular aromatic cores that adopt a nearly vertically packing mode (Fig. 5c and Fig. S13d, ESI†). From the supramolecular point view, the **DPAF-8** molecular arrangement in the crystal has obviously helical features. Therefore, the molecular chains in Fig. 5b and c may pack into wires with twisted or helical characteristic. For molecules **DPAF-12** and **DPAF-16** with longer flexible alkyl chains, the twisted or helical architectures should be more easily generated based on supramolecular assembly.<sup>16</sup> Single crystal analysis demonstrated a possible explanation for the formation mechanism of twisted wires in this study.

In conclusion, three **DPAF-*n*** ( $n = 8, 12, 16$ ) with identical central aromatic cores and different lengths of flexible alkyl chains have been synthesized and employed as building blocks to fabricate 1D nano/micro-structures. It was

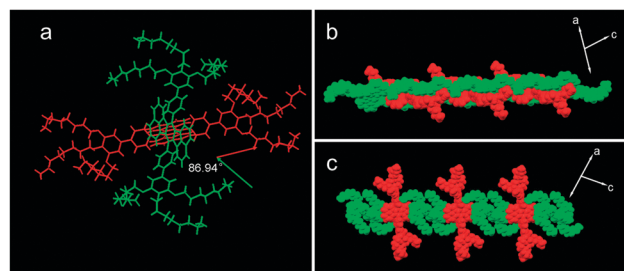


**Fig. 5** Molecular packing in **DPAF-8** crystal structures: (a) view of the molecules arrangement in twisted form along the ac axial plane; (b) the molecular chains observed along  $[10\bar{1}]$  direction under space fill style; (c) the molecular chains observed along  $[101]$  direction under space fill style.

demonstrated that 1D luminescent twisted wires were achieved based on **DPAF-*n***. Compared with **DPAF-8** and **DPAF-16**, **DPAF-12** molecules displayed stronger twisted aggregation property and could assemble into a 1D twisted structure under wide phase transfer conditions. The **DPAF-12** based wires with twisted and straight morphologies presented different emission characteristics, which were attributed to the different molecular packing in the 1D structures. Single crystal X-ray studies revealed supramolecular helical structural features in a **DPAF-8** crystal, which should be the driving force to induce the formation of a twisted structure in this study.

This work was supported by the National Natural Science Foundation of China (91333201, 51173065 and 21221063) and the Program for Chang Jiang Scholars and Innovative Research Team in University (No. IRT13018).

## Notes and references

- (a) A. E. Rowan and R. J. M. Nolte, *Angew. Chem., Int. Ed.*, 1998, **37**, 63–68; (b) A. R. A. Palmans and E. W. Meijer, *Angew. Chem., Int. Ed.*, 2007, **46**, 8948–8968.
- (a) J. H. Fuhrhop and W. Helfrich, *Chem. Rev.*, 1993, **93**, 1565–1582; (b) W. Li, J. Li and M. Lee, *Chem. Commun.*, 2013, **49**, 8238–8240.
- T.-F. Lin, R.-M. Ho, C.-H. Sung and C.-S. Hsu, *Chem. Mater.*, 2008, **20**, 1404–1409.
- (a) F. D. Maria, P. Olivelli, M. Gazzano, A. Zanelli, M. Biasiucci, G. Gigli, D. Gentili, P. D'Angelo, M. Cavallini and G. Barbarella, *J. Am. Chem. Soc.*, 2011, **133**, 8654–8661; (b) M. Yamauchi, S. Kubota, T. Karatsu, A. Kitamura, A. Ajayaghosh and S. Yagai, *Chem. Commun.*, 2013, **49**, 4941–4943.
- M. Goh, M. Kyotani and K. Akagi, *J. Am. Chem. Soc.*, 2007, **129**, 8519–8527.
- (a) H. Ozawa, H. Tanaka, M. Kawao, S. Uno and K. Nakazato, *Chem. Commun.*, 2009, 7411–7413; (b) Q. Zhao, Y. Wang, Y. Qiao, X. Wang, X. Guo, Y. Yan and J. Huang, *Chem. Commun.*, 2014, **50**, 13537–13539.
- (a) D. Ke, A. Tang, C. Zhan and J. Yao, *Chem. Commun.*, 2013, **49**, 4914–4916; (b) X. Zhang, D. Görl, V. Stepanenko and F. Würthner, *Angew. Chem.*, 2014, **126**, 1294–1298; (c) E. Yue, X. Ma, Y. Zhang, Y. Zhang, R. Duan, H. Ji, J. Li, Y. Che and J. Zhao, *Chem. Commun.*, 2014, **50**, 13596–13599.
- Y. Zhao, Y. Fan, X. Mu, H. Gao, J. Wang, J. Zhang, W. Yang, L. Chi and Y. Wang, *Nano Res.*, 2009, **2**, 493–499.
- (a) T. Yamamoto, T. Fukushima, A. Kosaka, W. Jin, Y. Yamamoto, N. Ishii and T. Aida, *Angew. Chem., Int. Ed.*, 2008, **47**, 1672–1675; (b) Y. Duan, S. Yan, X. Zhou, W. Xu, H. Xu, Z. Liu, L. Zhang, C. Zhang, G. Cui and L. Yao, *Chem. Commun.*, 2014, **50**, 8335–8338; (c) H. Cao, Q. Yuan, X. Zhu, Y. P. Zhao and M. Liu, *Langmuir*, 2012, **28**, 15410–15417.
- N. Giuseppone, J.-L. Schmitt and J.-M. Lehn, *J. Am. Chem. Soc.*, 2006, **128**, 16748–16763.
- (a) D. González-Rodríguez, J. L. J. van Dongen, M. Lutz, A. L. Spek, A. P. H. J. Schenning and E. W. Meijer, *Nat. Chem.*, 2009, **1**, 151–155; (b) G. Chen and M. Jiang, *Chem. Soc. Rev.*, 2011, **40**, 2254–2266; (c) S. Matile, A. V. Jentzsch, J. Montenegro and A. Fin, *Chem. Soc. Rev.*, 2011, **40**, 2453–2474.
- L. Chen, K. S. Mali, S. R. Puniredd, M. Baumgarten, K. Parvez, W. Pisula, S. D. Feyter and K. Mullen, *J. Am. Chem. Soc.*, 2013, **135**, 13531–13537.
- (a) E. F. Fabrizio, I. Prieto and A. J. Bard, *J. Am. Chem. Soc.*, 2000, **122**, 4996–4997; (b) M. Wehmeier, M. Wagner and K. Müllen, *Chem. – Eur. J.*, 2001, **7**, 2197–2205; (c) K. Matuszná, V. Lukeš, P. Rápta, L. Dunsch, A. J. A. Aquino and H. Lischka, *Synth. Met.*, 2007, **157**, 214–221; (d) L. Duan, D. Zhang, K. Wu, X. Huang, L. Wang and Y. Qiu, *Adv. Funct. Mater.*, 2011, **21**, 3540–3545; (e) B. F. Plummer, L. K. Steffen, T. L. Braley, W. G. Reese, K. Zych, G. Van Dyke and B. Tulle, *J. Am. Chem. Soc.*, 1993, **115**, 11542–11551.
- (a) Z. Zhang, Y. Zhang, D. Yao, H. Bi, I. Javed, Y. Fan, H. Zhang and Y. Wang, *Cryst. Growth Des.*, 2009, **9**, 5069–5076; (b) K. Wang, H. Zhang, S. Y. Chen, G. C. Yang, J. B. Zhang, W. J. Tian, Z. M. Su and Y. Wang, *Adv. Mater.*, 2014, **26**, 6168–6173.
- (a) J. Wang, Y. Zhao, J. Zhang, J. Zhang, B. Yang, Y. Wang, D. Zhang, H. You and D. Ma, *J. Phys. Chem. C*, 2007, **111**, 9177–9183; (b) Y. Zhao, X. Mu, C. Bao, Y. Fan, J. Zhang and Y. Wang, *Langmuir*, 2009, **25**, 3264–3270.
- C. Dou, D. Li, H. Zhang, H. Gao, J. Zhang and Y. Wang, *Sci. China: Chem.*, 2011, **54**, 641–650.